

Formation of an Alignment in Collisions of Laser Excited Sodium with Xenon Atoms

M. Elbel, H. Hühnermann, Th. Meier and W. B. Schneider

Fachbereich Physik, Universität Marburg, Germany

Received September 18, accepted September 26, 1975

Abstract. By photon absorption from a monomode dye-laser beam a spatially ordered velocity distribution ('atomic beam') of sodium atoms excited to the $3p^2P_{1/2}$ -state, is created. It is predicted theoretically that in collisions of these atoms with atoms of a heavy foreign gas an alignment of the electronic orbital angular momentum is produced. This alignment leads to the appearance of a linear polarization in the sensitized D_2 -fluorescent light. This polarization is verified experimentally and interpreted in terms of a simplified T -operator. It turns out that the scattering distribution for sensitizing collision is of the wide-angle type.

I. Introduction

It is well known and has been treated in many a textbook that in electron-atom collisions excitation is brought about and that, in particular, the excited state of the atom is produced in an aligned manner so that the angular momentum of the excited atom proves to be oriented at the k -vector (relative velocity) of the colliding pair. It ought not surprise, therefore, if in atom-atom collisions such an effect were likewise present. Experimentally this could be easily proved if at least one of the atoms pertains to an atomic beam rather than a random velocity distribution (e.g. gas or vapour) and if at least one of the atoms changes state during the collision giving rise to the appearance of a photon when decaying back to the initial state. The spatial distribution and polarization of the emitted photon allows then the determination of the alignment of the decaying state. An experiment which refers to this was successfully carried through by Kempter and Mecklenbrauck [1] who used a potassium atomic beam at suprathreshold energies (100...1.000 eV) to excite the $4p^2P_{3/2}$ -state in collisions with thermal argon atoms. Evidently, atomic beams at thermal energies are not suited for similar experiments because of the energy threshold represented by the crossing of the $4s$ and $4p$ energy curves

at several 10 eV in which the transformation of the states occurs.

However, thermal energies were sufficient in sensitizing collisions of excited atoms. Starting with sodium atoms in the $3p^2P_{1/2}$ -state which are necessarily disaligned, a sizeable fraction of them may change to the $3p^2P_{3/2}$ -state during collisions with noble gas atoms. The latter state during decay emits D_2 -photons which may turn out to be linearly polarized with respect to the k -vector. If the k -vector is spatially randomized which is so when both collision partners pertain to random velocity distributions, then the polarization of the photons is averaged to zero. A net polarization remains solely if at least one of the colliding partners pertains to an atomic beam or some other directed velocity distribution. One might think of an atomic beam of sodium atoms which are excited while traversing a gas target of noble gas atoms. This idea has to be discarded because the excited state $3p^2P_{1/2}$ is so short-lived that in order to obtain sizeable collision rates during the life time, one has to choose the density of the gas target high to the degree that the sodium beam were spatially randomized before entering the region where excitation occurs. How to form, then, an atomic beam of excited atoms? The

answer was given in a proposal by Pritchard and Phillips [2]. Utilize narrow-banded excitation which is rendered possible by a dye laser. The laser frequency ν may be tuned to some point on the wing of the Doppler-profile of the D_1 -line whose centre-frequency be ν_0 . Only those atoms are excited which move along the laser beam with such a velocity component v_z that

$$\frac{v_z}{c} = \frac{\nu - \nu_0}{\nu_0} \quad (1)$$

The laser does not select the velocity components v_x, v_y which are perpendicular to the beam, so that the distribution of those components remains Maxwellian. But the spatial distribution of the v -vector when represented in the form of a polar diagram is no longer random. It is disc-shaped when the laser is tuned to the centre frequency. It approaches more and more the form of a cone pointed parallel or antiparallel along the laser beam when the laser is detuned to the blue or red wing of the line. The problem how an apparent alignment of the atomic velocities is transformed by collisions into an alignment of the atomic angular momenta deserves a little more intense discussion before presenting the outline and result of a respective experiment.

II. Creation of an Alignment in Sensitizing Collisions

A considerable number of articles [3-6] was devoted to the purpose of calculating the transition probabilities among the entire set of Zeeman substates of sodium $3p$ doublet. The aim to deduce a comprehensive transition operator which accounts for all of these, is not yet attained. It was yet shown [7] that there are two prevailing terms

$$\mathcal{F}(\mathbf{k}, \mathbf{k}') = c_2 (\mathcal{L}^{(2)} \cdot \mathbf{C}^2(\mathbf{k} - \mathbf{k}')) + c_1 (\mathcal{L}^{(1)} \cdot \mathbf{C}^1(\mathbf{k} \times \mathbf{k}')) + \dots \quad (2)$$

where

$$\mathcal{L}^{(1)} = (\mathcal{L}_x^{(1)}, \mathcal{L}_y^{(1)}, \mathcal{L}_z^{(1)}) \quad (2a)$$

$$\mathcal{L}_0^{(1)} = \mathcal{L}_z, \quad \mathcal{L}_{\pm 1}^{(1)} = \mp \frac{1}{\sqrt{2}} (\mathcal{L}_x \pm i \mathcal{L}_y) \quad (2b)$$

and $\mathcal{L}^{(2)}$ is built on the components of $\mathcal{L}^{(1)}$ according to Eq. (2c)

$$\mathcal{L}_r^{(2)} = \sum_{p+q=r} (1p1q|112r) \mathcal{L}_p^{(1)} \mathcal{L}_q^{(1)} \quad (2c)$$

Here $\mathcal{L} \equiv (\mathcal{L}_x, \mathcal{L}_y, \mathcal{L}_z)$ denotes the vector operator of the electronic orbital angular momentum, $\mathbf{C}^{(2)}(\mathbf{k} - \mathbf{k}')$ the standard tensor of second degree

depending on the angular coordinates of the transferred momentum vector $\mathbf{k} - \mathbf{k}'$ of the colliding atoms. $\mathbf{C}^{(1)}(\mathbf{k} \times \mathbf{k}')$ the standard tensor of first degree depending on the angular coordinates of the vector $\mathbf{k} \times \mathbf{k}'$ which stands perpendicularly on the scattering plane. The coordinate system is arbitrarily chosen. It has been made evident, mostly by the study of polarization transfer between the $3p^2P_{1,2}$ and the $3p^2P_{3,2}$ state [8], that the first term in Eq. (2) is by far the leading one: $c_2 \gg c_1$. We therefore neglect all terms beside the first one in Eq. (2) in the following discussion.

If we choose for the moment the vector $\mathbf{k} - \mathbf{k}'$ as the z -axis of our system then the T -operator (first term only) assumes the form

$$= c_2 \mathcal{L}_0^{(2)}. \quad \mathbf{C}_0^2(\vartheta=0, \varphi) = c_2 \mathcal{L}_0^{(2)}. \quad (3)$$

Consider that the laser beam populates the sublevels $m_j = +1/2$ and $m_j = -1/2$ of $3p^2P_{1,2}$ through pure σ -excitation, incoherently at equal rates. From these levels through the T -operator Eq. (2) only the levels $m_j = \pm 1/2$ of the final state $3p^2P_{3,2}$ are reached. Levels $m_j = \pm 3/2$ are left empty. Such a population in the state $3p^2P_{3,2}$ gives rise to a strong alignment: Al. One easily verifies

$$\text{Al} = N_{j=3,2} \langle J_0^{(2)} \rangle_{j=3,2, z \parallel \mathbf{k} - \mathbf{k}'} = \frac{\langle 3J_z^2 - J^2 \rangle_j}{j(2j-1)} \Big|_{j=3,2} = -1. \quad (4)$$

Here $J_0^{(2)}$ consists of the components of the angular momentum operator \mathbf{J} as indicated by Eq. (2c). j is the quantum number pertinent to J . N_j is a normalizing factor defined by

$$N_j = 1 / \langle j, m_j = j | J_0^{(2)} | j, m_j = j \rangle. \quad (4a)$$

We are interested in an alignment referred to the \mathbf{k} -axis rather than the $\mathbf{k} - \mathbf{k}'$ -axis. Consequently, we have to project the alignment Eq. (4) on the \mathbf{k} -axis. Let ϑ', φ' be the scattering angles

$$\varphi' = \angle(\mathbf{k} \times \mathbf{k}', y); \quad \vartheta' = \angle(\mathbf{k}, \mathbf{k}'). \quad (5)$$

It then follows that

$$\angle(\mathbf{k}, \mathbf{k} - \mathbf{k}') = \frac{\pi - \vartheta'}{2} \quad (6)$$

provided the collision process can be considered as elastic. This, in turn, appears to be a good assumption since the mean kinetic energy of the colliding partners at room temperature exceeds the energetic deficiency of the $3p^2P$ -levels (~ 2 meV) by more than an order

of magnitude. Thus we have

$$\langle J_q^{(2)} \rangle_{j=3,2, \mathbf{k} \parallel z} = D_{0,q}^{(2)} \left(-\psi', \frac{\vartheta'}{2}, -\frac{\pi}{2}, -\varphi' \right) \langle J_0^{(2)} \rangle_{j=3,2, \mathbf{k} - \mathbf{k}' \parallel z} \quad (7)$$

where $\varphi', \frac{\pi - \vartheta'}{2}, \psi'$ is the eulerian triple which is swept out when rotating the original system with $z \parallel \mathbf{k} - \mathbf{k}'$ into its new position with $z \parallel \mathbf{k}$. The alignment components $\langle J_q^{(2)} \rangle_{\mathbf{k} \parallel z}$ are to be averaged over the scattering distribution $d\sigma/d\Omega$ to obtain the alignment which can be observed experimentally. Since $d\sigma/d\Omega$ does not depend on the azimuth φ' all components $\langle J_q^{(2)} \rangle$ cancel except when $q=0$. Hence we have

$$\begin{aligned} \overline{\langle J_0^{(2)} \rangle_{j=3,2, \mathbf{k} \parallel z}} &= \frac{1}{\sigma} \int_0^{2\pi} \int_0^{\pi} \left(3 \cos^2 \left(\frac{\pi - \vartheta'}{2} \right) - \frac{1}{2} \right) \frac{d\sigma}{d\Omega}(\vartheta') \cdot \sin \vartheta' d\vartheta' d\varphi' \\ &= \frac{1}{\sigma} \int_0^{2\pi} \int_0^{\pi} \left(3 \sin^2 \frac{\vartheta'}{2} - \frac{1}{2} \right) \frac{d\sigma}{d\Omega}(\vartheta') \cdot \sin \vartheta' d\vartheta' d\varphi' \\ &= \frac{1}{\sigma} \int_0^{2\pi} \int_0^{\pi} \frac{1 - 3 \cos \vartheta' d\sigma}{4} \frac{d\sigma}{d\Omega}(\vartheta') \cdot \sin \vartheta' d\vartheta' d\varphi'. \end{aligned} \quad (8)$$

It therefore appears that the alignment relative to the \mathbf{k} -axis is closely connected with the dipolar momentum of the scattering distribution. The study of the alignment, accordingly, gives a first hint at the details of the scattering distribution.

Let us consider two important examples of atomic scattering distributions.

i) Isotropic Scattering

The scattering distribution is given as

$$\frac{d\sigma}{d\Omega} = \frac{\sigma}{4\pi}. \quad (9)$$

Result:

$$N_{j=3,2} \overline{\langle J_0^{(2)} \rangle_{j=3,2, \mathbf{k} \parallel z}} = \frac{1}{4} N_{j=3,2} \langle J_0^{(2)} \rangle_{j=3,2, z \parallel \mathbf{k} - \mathbf{k}'} = -\frac{1}{4}. \quad (9a)$$

ii) Extreme Forward Scattering

$$\frac{d\sigma}{d\Omega} = \frac{\sigma}{2\pi} \cdot \delta(\cos \vartheta', 1). \quad (10)$$

Result:

$$\begin{aligned} N_{j=3,2} \overline{\langle J_0^{(2)} \rangle_{j=3,2, \mathbf{k} \parallel z}} &= -\frac{1}{2} N_{j=3,2} \langle J_0^{(2)} \rangle_{j=3,2, z \parallel \mathbf{k} - \mathbf{k}'} = \frac{1}{2}. \end{aligned} \quad (10a)$$

It has been suggested that a realistic approach to the atomic scattering distribution consists in an approximately equal sharing of isotropic scattering and

forward scattering (cf. Massey [9]). Then the sum of the alignments predicted in i) and ii) were to be expected, i.e.

$$N_{j=3,2} \overline{\langle J_0^{(2)} \rangle_{j=3,2, \mathbf{k} \parallel z}} \cong +\frac{1}{4}. \quad (11)$$

In planing an experimental determination of $\langle J_0^{(2)} \rangle$ we recall from the introduction that by Doppler-shifted excitation with laser light it is not possible to get the velocity vector \mathbf{v} completely aligned.

We can only achieve a non-thermal distribution which is axially symmetric to the laser beam. Moreover, the vector \mathbf{v} does not coincide with the vector \mathbf{k} as the latter is proportional to the relative velocity \mathbf{v}_r to which the velocity vectors of both collision partners contribute. However, we have at our disposal to choose such a heavy collision partner (e.g. xenon) that its proper motion may be neglected against the one of the excited sodium atom. But even so, we are left with projecting the alignment which until now was referred to \mathbf{k} , upon the laser beam. Let us assume that \mathbf{v} were parallel to \mathbf{k} . The vector \mathbf{v} and the laser beam for one particular atom may include the angle Θ , then

$$\langle J_0^{(2)} \rangle_{j=3,2, z \parallel \text{laser beam}} = \left(\frac{3}{2} \cos^2 \Theta - \frac{1}{2} \right) \langle J_0^{(2)} \rangle_{j=3,2, z \parallel \mathbf{k}} \quad (12)$$

where

$$\cos \Theta = \frac{v_z}{v} \quad (13)$$

$$v = (v_x^2 + v_y^2 + v_z^2)^{1/2}. \quad (13a)$$

In Eq. (13) v_z is determined by the laser frequency through Eq. (1). The velocity components v_x and v_y obey Maxwell distributions. The projecting multiplier in Eq. (12) has to be averaged over the distributions of v_x and v_y

$$\begin{aligned} &\overline{\left(\frac{3}{2} \cos^2 \Theta - \frac{1}{2} \right) v_x v_y} \\ &= \frac{m}{2\pi k T} \int_{-\infty}^{\infty} \int_{-\infty}^{\infty} \left(\frac{3v_z^2}{2(v_x^2 + v_y^2 + v_z^2)} - \frac{1}{2} \right) \\ &\cdot \exp \left(-\frac{m}{2} \frac{v_x^2 + v_y^2}{k T} \right) dv_x dv_y, \\ &= -\frac{3}{2} \frac{m v_z^2}{2k T} \exp \left(\frac{m v_z^2}{2k T} \right) E_i \left(-\frac{m v_z^2}{2k T} \right) - \frac{1}{2}. \end{aligned} \quad (14)$$

Here m denotes the mass of the sodium atom. $E_i(x)$ is the exponential integral function which is tabulated e.g. in [10]. This function for negative argument assumes negative values so that the first term in Eq. (3) is always positive. Fig. 1 displays the averaged projecting multiplier Eq. (13) as a function of

$$u = \left| \frac{m}{2k T} v_z \right| = \left| \frac{m}{2k T} c \frac{v - v_0}{v_0} \right|. \quad (15)$$

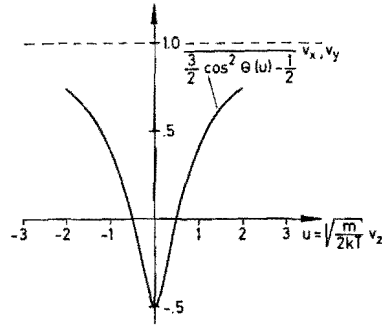


Fig. 1. The projection multiplier Eq. (14) as a function of the normalized z -component of the velocity Eq. (15). Broken line: Limit for large u -values

Note that the alignment in the line centre takes on half the value it has on the far wings while the sign is opposite. Hence and from Eq. (9a) we expect an alignment of -12.5% in the line centre. If a nuclear spin is present part of this alignment may turn into a nuclear alignment through hyperfine interaction. Hence it escapes detection. Fortunately, for sodium $l=j=3/2$ so that the created alignment is equally partitioned among both spin systems. The value in the line centre is then further reduced to -6.25% . Hence we cannot expect spectacular experimental effects.

The alignment referred to the laser-beam axis is detected from unequal amounts of σ -quanta and π -quanta, I_σ and I_π , which are emitted from the $3p^2P_{3/2}$ -state at right angles to the laser beam. Then the following relation holds [11]

$$I_\sigma - I_\pi \propto n_{3/2} \cdot \langle J_0^{(2)} \rangle_{j=3/2, z \parallel \text{laser beam}} \quad (16)$$

The expected signal follows from the average alignment. Fig. 1, by multiplying with the population of the state $3p^2P_{3/2}; n_{3/2}$. The latter quantity depends on the frequency ν of the exciting light like a Doppler curve: $f_D(u) = \exp(-u^2)$, hence

$$I_\sigma - I_\pi \propto -\frac{3}{2} u^2 E i(-u^2) - \frac{1}{2} \exp(-u^2). \quad (17)$$

This function together with $f_D(u)$ is displayed in Fig. 2. The signal $I_\sigma - I_\pi$ in comparison to the excitation rate is expected to show a distinctly reduced width aside from its inverted form. If the fluorescent line consists of several hyperfine components then any component should exhibit the form of Fig. 2. So much for the predictions of the theory which are now to be checked experimentally!

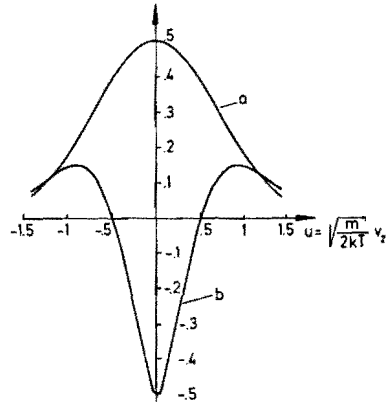


Fig. 2. Curve a: Doppler distribution arbitrarily normalized to 0.5. Curve b: Predicted signal $I_\sigma - I_\pi$ according to Eq. (17). This shape pertains to a spectral line which shows, by hypothesis, no hyperfine structure

III. Experimental

A laser beam from a dye laser (Spectra Physics Model 580) which was tuned to the sodium D_1 -line $\lambda = 5,896 \text{ \AA}$, was made incident on a sodium vapour. The sodium vapour was kept in a sealed-off pyrex cell at 100°C shaped like a Wood's horn, together with a few tenths of a Torr of xenon. The fluorescent D_2 -light $\lambda = 5,890 \text{ \AA}$ which was sensitized by sodium xenon collisions, was observed at right angles to the laser beam. The light at first was transmitted through a rotating linear analyzer and then was focussed on the entrance slit of a 1m -Czerny-Turner spectrograph which served to resolve the D -lines. A photomultiplier with an ERMA photokathode was used for detection and the electric signal was then rectified sensitively to the phase of a signal from a photodiode which was illuminated by a reference light beam. The latter was periodically interrupted by a shutter which was rigidly connected with the rotating linear analyzer (cf. Fig. 3).

The rotating analyzer had to fulfill the demand that the polarization plane of the transmitted light should not rotate but keep its orientation. This demand was imposed by the spectrograph which had strongly polarizing properties. Otherwise the spectrograph would have produced a spurious alternating signal. Therefore the first rotating circular polarizer transformed linear polarized light of varying plane into circularly polarized light whereas the second standing circular analyzer transformed the circularly polarized light back into linear polarized light of rigid plane.

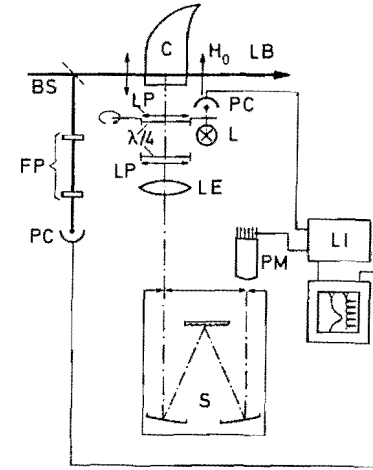


Fig. 3. Experimental arrangement. LB Single mode laser beam. The polarization was in the drawing plane as indicated. C Resonance cell with sodium vapour and 1 Torr xenon. LP Linear polarizer. $\lambda/4$ Quarter wave plate. LE Lens. S Spectrograph. PM Photomultiplier. LI Lock-in set. L Lamp. PC Photocell. BS Beam splitter. FP Fabry-Pérot interferometer. The steady magnetic field H_0 served for depolarizing the signal. 21Oe were sufficient to reduce the signal to one half if the xenon pressure was chosen 0.5 Torr

The rectified signal was recorded by a multi-channel strip-chart recorder which at another channel recorded interferences produced by an FP-interferometer and a photodiode. The interferences served as frequency marks.

The dye laser was operated in a single mode whose spectral purity was controlled by the FP-interferometer. The laser beam scanned a frequency range of $4\text{GHz} = 133\text{ mK}$. The scanning was attained by continuously changing the cavity length. Mode-jumping was prevented by automatically tuning the maximum of the response curve of the intracavity etalon to the lasing mode of the cavity.

To prove the absence of any spurious polarization in the detecting beam at the outset of any experiment the sodium vapour was excited with D_2 -light and the sensitized D_1 -light was checked to be unpolarized. Afterwards the adjustments of the laser beam and the spectrograph were reverted with respect to the lines and a recording of the difference of the sensitized $D_2 \sigma$ -light and $D_2 \pi$ -light, $I_\sigma - I_\pi$, was taken while the laser scanned the absorption profile. Such a signal was not found with 1 Torr neon as a buffer gas. Then the linear polarizer which during this run was situated in front of the entrance slit of the spectrograph, was removed and placed between cell and circular polarizer.

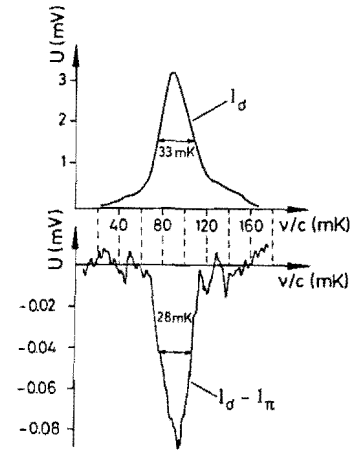


Fig. 4. The recorded signal I_σ (upper part) and $I_\sigma - I_\pi$ (lower part of the drawing). The sensitivity differs by a factor of 50 between both parts. The xenon pressure was 1 Torr, the temperature of the cell 110°C

This enabled us to measure the σ -component, I_σ , of the D_2 -light alone. Two recordings taken in that manner are shown in Fig. 4. From these recordings we deduced the maximum alignment to be 1.6% for a xenon pressure of 1.0 Torr.

In doing so the relation

$$A1 = \frac{(I_\sigma - I_\pi)_{90^\circ}}{(I_\sigma + \frac{1}{2} I_\pi)_{90^\circ}} \quad (18)$$

which has been proved for example in Ref. 11, was used.

Although the magnitude of the measured alignment meets the prediction of Section II, we do not understand some other details of the recording e.g.

- Why is the signal $I_\sigma - I_\pi$ dissimilar to the predicted shape in Fig. 1 in particular, why is there no trace of an inversion?
- Why does the signal I_σ not show any trace of a hyperfine structure? Moreover, why is the half-width much lower than the hyperfine splitting of the ground state $3s^2S_{1/2}$, 59 mK, and even lower than the Doppler half-width, 50 mK?
- Why is the half-width of $I_\sigma - I_\pi$ reduced to about three quarters of the half-width of I_σ ?

These problems are clarified by considering the influence of optical pumping on the excitation process.

IV. Optical Pumping and Laser Excitation

As emphasized by other authors, cf. Ref. 12, optical pumping exerts an important influence on the laser

excitation process. But to our knowledge this influence was exclusively studied at low atomic densities. In our case a dense foreign gas is present so that a definite atom which initially fulfills the resonance condition, after one absorption-emission process would have no chance to go through another one. Instead, when back to the ground state it instantaneously would suffer a collision which would change its velocity vector and accordingly, destroy the resonance condition. The place in the velocity distribution the former atom has left would be taken by another atom which is scattered into the resonant state of motion. Again it would go through an absorption-emission process and, by renewed scattering, leave its place to a third one. At these conditions hole-burning does not occur. Accordingly all the atoms in the velocity distribution through strong collisional coupling of all the states of motion, have an equal chance of absorption. The rate at which they are excited, is proportional to the number of atoms per velocity interval at the resonant velocity component v_2 according to Eq. (1). Hence it conforms to a Doppler distribution. In the sodium ground state there are two hyperfine sublevels: $F=1$ and $F=2$. Neglecting for the moment the splitting of the excited state, there are two Doppler distributions centred at v_1 and v_2 for the atoms in state $F=1$ and $F=2$. Tuning for instance the laser to v_2 it is clear that by far more atoms are excited from state $F=2$ than from state $F=1$. After decay a much larger number of atoms has changed from state $F=2$ to state $F=1$ than in the counter direction. Accordingly, the state $F=2$ is depleted and the state $F=1$ is replenished. The redistributing process ends when a new equilibrium is reached such that the rates of atoms which change their state in both ways during an absorption-emission cycle become equal. The net absorption rate by this redistributing process is very much reduced. One easily imagines that the distributions of $F=1$ atoms and $F=2$ atoms are least disturbed when the laser is tuned

$$E(v; v_1, v_2, \delta v_D) = \frac{3 \exp\left(\frac{(v-v_1)^2 - (v-v_2)^2}{\delta v_D^2}\right) \exp\left(-\frac{(v-v_1)^2}{\delta v_D^2}\right) + 5 \exp\left(-\frac{(v-v_2)^2}{\delta v_D^2}\right)}{3 \exp\left(\frac{(v-v_1)^2 - (v-v_2)^2}{\delta v_D^2}\right) + 5} \quad (21)$$

to some frequency between v_1 and v_2 . We therefore expect the excitation curve to have its maximum at some place between v_1 and v_2 . To see that in more detail let us write down rate equations. We use abbreviations n_1, n_2 for the $F=1, 2$ -population numbers in the ground state $3s^2S_{1/2}$, N_1, N_2 for the excited $3p^2P_{1/2}$ state, respectively. The excited state splitting of 6.3 mK is neglected for simplicity. v denotes the

laser frequency, δv_D the Doppler width. δv_D equals 30 mK at our conditions, which corresponds to a half-width of 50 mK. Only optical excitation and emission are taken into consideration. I stands for the flux of photons, σ for the absorption cross section. τ is the mean life of the excited state. Relative optical transition probabilities are given numerically.

$$\dot{n}_1 = -I\sigma \exp\left(-\left(\frac{v-v_1}{\delta v_D}\right)^2\right) n_1 + \frac{1}{6} \frac{N_1}{\tau} + \frac{1}{2} \frac{N_2}{\tau} \quad (19a)$$

$$\dot{n}_2 = -I\sigma \exp\left(-\left(\frac{v-v_2}{\delta v_D}\right)^2\right) n_2 + \frac{5}{6} \frac{N_1}{\tau} + \frac{1}{2} \frac{N_2}{\tau} \quad (19b)$$

$$\dot{N}_1 = \frac{1}{6} I\sigma \exp\left(-\left(\frac{v-v_1}{\delta v_D}\right)^2\right) n_1 + \frac{1}{2} I\sigma \exp\left(-\left(\frac{v-v_2}{\delta v_D}\right)^2\right) n_2 - \frac{N_1}{\tau} \quad (19c)$$

$$\dot{N}_2 = \frac{5}{6} I\sigma \exp\left(-\left(\frac{v-v_1}{\delta v_D}\right)^2\right) n_1 + \frac{1}{2} I\sigma \exp\left(-\left(\frac{v-v_2}{\delta v_D}\right)^2\right) n_2 - \frac{N_2}{\tau} \quad (19d)$$

When slowly scanning the absorption profile we can confine ourselves to discussing the stationary solution of these equations. We find them to be

$$\frac{n_1}{n_2} = \frac{3}{5} \exp\left(\frac{(v-v_2)^2 - (v-v_1)^2}{\delta v_D^2}\right) = \frac{3}{5} \exp\left(2(v_2 - v_1)\left(v - \frac{v_1 + v_2}{2}\right) / \delta v_D^2\right) \quad (20)$$

This and the constraint

$$n_1 + n_2 = \text{const}$$

which is justified so long as $n_1, n_2 \gg N_1, N_2$, allows one to calculate the excitation rate:

After putting the origin of the frequency scale to the mean frequency of the hyperfine structure, i.e. introducing the variable

$$x = v - \frac{v_1 + v_2}{2} \quad (22)$$

and, as a parameter,

$$hfs = v_1 - v_2 \quad (23)$$

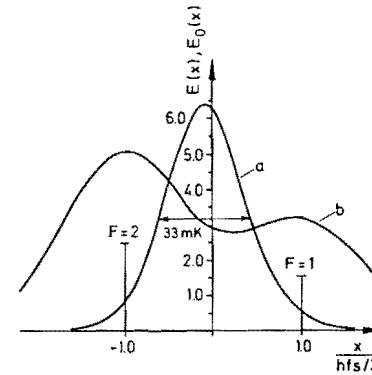


Fig. 5. Excitation curves. The case of Curve a: Strong optical pumping between both hyperfine sublevels of the ground state. $E(x; hfs, \delta v_D)$ according to Eq. (24) is displayed. Curve b: Optical pumping is ineffective. $E_0(x; hfs, \delta v_D)$ according to Eq. (25) is displayed. The curves are equally valid for D_1 and D_2 light pumping

Eq. (21) is transformed after short calculation into

$$E(x; hfs, \delta v_D) = \frac{\exp\left(-\frac{x^2}{\delta v_D^2}\right)}{\frac{3}{4} \cosh\left(\frac{hfs \cdot x}{\delta v_D^2}\right) + \frac{1}{4} \sinh\left(\frac{hfs \cdot x}{\delta v_D^2}\right)} \quad (24)$$

In Fig. 5 the function $E(x; hfs, \delta v_D)$ is displayed along with the excitation curve which we would expect if optical pumping were ineffective: $E_0(x; hfs, \delta v_D)$:

$$E_0(x; hfs, \delta v_D) = \frac{3}{8} \exp\left(-\left(\frac{x - \frac{hfs}{2}}{\delta v_D}\right)^2\right) + \frac{5}{8} \exp\left(-\left(\frac{x + \frac{hfs}{2}}{\delta v_D}\right)^2\right) \quad (25)$$

The striking reduction of the half-width from the Doppler value 50 mK to 33 mK (calculated) becomes apparent.

To render possible a comparison with experiment excitation curves were taken under different conditions. We successively used cells with and without buffer gas and at one instance we reflected the laser beam back in itself. The curves obtained for D_2 -excitation are shown in Fig. 6. The laser power was 5 mW which was too low to provide conditions of saturation spectroscopy but, without buffer gas and with the beam reflected, we observed pumping holes and spikes in the excitation curve [12]. The two holes marked the transition frequencies v_1 and v_2 in a welcome manner and thus rendered possible frequency calibration.

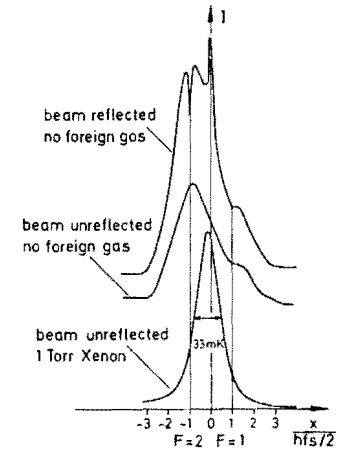


Fig. 6. A few recorded excitation curves. D_2 -light was likewise used for excitation and detected. The fluorescence from the gasfilled cell was then times more intense than from the cell without foreign gas

The spike, in turn, results from atoms which are in such a state of motion that they are at resonance with the original laser beam when in the $F=1$ -state and with the reflected laser beam when in the $F=2$ -state. For these atoms pumping is inhibited and, accordingly, the absorption rate is much enhanced. The spike marks the mean transition frequency and thus the origin of the x-scale. The scales of the three excitation curves were comparable owing to the fringes of the FP -interferometer in the branched-off beam (not shown). The reduction in width of the excitation curve to 33 mK is demonstrated as well as the slight shift (3 mK) towards the $F=2$ -transition frequency. There is one final point left to explanation. It concerns the shape of the alignment signal. We understand now that in its production two processes interfere; namely optical pumping and velocity selection. The influence of optical pumping is given by Eq. (24), the one of velocity selection by Eq. (14). In particular, at a given laser frequency, we have to multiply the rate of atoms which is excited from state $F=1$, with the projection multiplier Eq. (14) centred at the frequency v_1 and to add the rate of atoms excited from state $F=2$ multiplied with the projection multiplier centred at v_2 . As is easily verified from Eq. (20), the ratio of the excitation rates from $F=1$ and $F=2$ is a constant (3 : 5), independent of the laser frequency, and the sum of both is given by Eq. (21). Accordingly, any of the rates is proportional to Eq. (21). The signal function

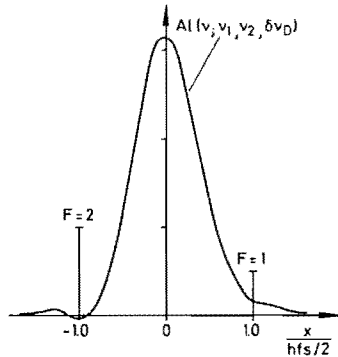


Fig. 7. The signal $I_\alpha - I_\pi$ as predicted from the theory which takes into account both velocity selection and optical pumping effects (Eq. (26))

which we will call $AI(v; v_1, v_2, \delta v_D)$, is therefore

$$\begin{aligned}
 & AI(v; v_1, v_2, \delta v_D) \\
 &= E(v; v_1, v_2, \delta v_D) \left[\frac{3}{8} \left(-\frac{3}{2} \frac{mc^2}{2kT} \left(\frac{v-v_1}{v_1} \right)^2 \right. \right. \\
 & \cdot \exp \left(\frac{mc^2}{2kT} \left(\frac{v-v_1}{v_1} \right)^2 \right) Ei \left(-\frac{mc^2}{2kT} \left(\frac{v-v_1}{v_1} \right)^2 \right) - \frac{1}{2} \right) \\
 & + \frac{5}{8} \left(-\frac{3}{2} \frac{mc^2}{2kT} \left(\frac{v-v_2}{v_2} \right)^2 \right. \\
 & \cdot \exp \left(\frac{mc^2}{2kT} \left(\frac{v-v_2}{v_2} \right)^2 \right) Ei \left(-\frac{mc^2}{2kT} \left(\frac{v-v_2}{v_2} \right)^2 \right) - \frac{1}{2} \right) \left. \right]. \quad (26)
 \end{aligned}$$

It is displayed in Fig. 7. There is hardly any similarity left to Fig. 2. The inverted shape of the latter curve has disappeared. On the other hand, the similarity with the experimental curve $I_\alpha - I_\pi$ in Fig. 4 is striking. Also the reduced half-width of the experimental curve (27 mK) is fully confirmed.

Our improved understanding of the alignment signal implies that the maximum does *not* coincide with the maximum of the projection multiplier $((3/2)\cos^2\vartheta - 1/2)^k$. It rather coincides with a frequency, call it v_M , for which $v_1 - v_M \approx v_M - v_2 \approx \delta v_D$. For $v = v_M$, the projection multiplier Eq. (14) is already inverted. Its value is +0.4 instead of -0.5 at the centre frequency. This and the fact that the signal $I_\alpha - I_\pi$ is negative leads to the conclusion that the scattering distribution of all the atoms which during scattering have made a transition from $^2P_{1/2}$ to $^2P_{3/2}$,

is not peaked into the forward direction. Isotropic scattering, however, would qualitatively fit into the finding. Indeed, the forward peak in scattering distributions is due to shape elastic scattering. It results from diffraction at the edge of the scattering obstacle. Hence it is not expected in inelastic scattering distributions like the one in question.

V. Conclusions

A prediction has been made that in collisions of excited sodium atoms which pertain to a spatially ordered velocity distribution, with heavy noble-gas atoms alignments may arise. The prediction was proved experimentally by preparing such a velocity distribution by laser excitation of the $3p^2P_{1/2}$ -state. Sensitized D_2 -light was detected. It was found to be linearly polarized which confirmed the prediction. The sign of the polarization indicated that the scattering distribution for sensitizing collisions is of the wide angle type.

Financial support of the Deutsche Forschungsgemeinschaft is gratefully acknowledged.

References

1. Kempster, V., Kübler, B., Mecklenbrauck, W.: J. Phys. B7, 2375 (1974)
- Alber, H., Kempster, V., Mecklenbrauck, W.: J. Phys. B8, 913 (1975)
2. Phillips, W.D., Pritchard, D.: Phys. Rev. Lett. 33, 1254 (1974)
3. Lewis, E.L., McNamara, L.F.: Phys. Rev. A5, 2643 (1972)
4. Masnou-Seeuws, F., Roueff, E.: Chem. Phys. Lett. 16, 593 (1972)
5. Reid, R.H.G.: J. Phys. B6, 2018 (1973)
6. Wilson, A.D., Shimoni, Y.: To appear in J. Phys. B
7. Elbel, M.: Z. Physik 248, 375 (1971)
8. Schneider, W.B.: Z. Physik 248, 387 (1971)
9. Massey, H.S.W.: Electronic and Ionic Impact Phenomena, Vol. III, Oxford At The Clarendon Press (1971)
10. Applied Mathematics Series 51, National Bureau of Standards, (1958)
11. Papp, J.F., Franz, F.A.: Phys. Rev. A5, 1763 (1972)
12. Hänsch, T.W., Shahin, I.S., Schawlow, A.L.: Phys. Rev. Lett. 27, 707 (1971)

Prof. Dr. M. Elbel
 Prof. Dr. H. Hühnermann
 Dr. Th. Meier
 Dr. W. B. Schneider
 Fachbereich Physik
 der Philipps-Universität Marburg
 D-3550 Marburg/Lahn
 Renthof 5
 Federal Republic of Germany